ARTICLE

Fluorescence and Electron Microscopic Localization of F-actin in the Ependymocytes

Yan-Chao Li, Wan-Zhu Bai, Kazuhisa Sakai, and Tsutomu Hashikawa

Neural Architecture, Advanced Technology Development Group, RIKEN Brain Science Institute, Saitama, Japan

SUMMARY The organization of F-actin in the ventricular system has been reported to display pronounced regional differences with respect to shape, size, and development. However, the real roles played by F-actin in these cells cannot be understood unless the precise localization of F-actin is defined. In the present study, we used double-fluorescence labeling to further examine the localization of F-actin in the ependymocytes and its spatial relation to the other two cytoskeletal components, microtubules and intermediate filaments. Then we converted fluorescence signals for F-actin to peroxidase/DAB reaction products by use of a phalloidin-based FITC-anti-FITC system. This detection technique provided an overview of the distribution of F-actin in the ependymocytes at the ultrastructural level, and has been proven to be helpful in correlating light and electron microscopic investigations.
(J Histochem Cytochem 57:741–751, 2009)

THE LUMINAL SURFACE of the ventricular system is covered by a single layer of cuboidal/columnar ependymocytes (Peters et al. 1991; Del Bigio 1995). The integrity of the ependyma is highly dependent on the unique organization of microfilaments. Disturbance of microfilaments results in partial or complete denudation of ependymocytes from the lining (Mestres and Garfia 1980; Koshiba 1987). Actin filaments (F-actin) are known as the main component of microfilaments. At the light microscopic level, either F-actin or actin proteins have been detected predominantly in the apical border of ependymocytes (Gröschel-Stewart et al. 1977; Ishii et al. 1978; Li et al. 2007,2008). This apical F-actin network displays pronounced regional differences with respect to shape, size, and development (Li et al. 2007,2008). However, because of the lack of precise localization, it is unclear what roles F-actin plays in the ependymocytes.

The apical surface of ependymocytes, like that of other epithelial cells, is covered with a varying number of cytoplasmic protrusions, such as cilia and microvilli. It is well known that microvilli contain a core of F-actin, which extends from the tips of microvilli downward into the apical cytoplasm and is anchored to a circumferential network of F-actin, the terminal web (Hirokawa et al. 1982; Hagen and Trier 1988). Although previous electron microscopic (EM) examinations have demonstrated the presence of microfilaments in the apical regions of ependymocytes (Brightman and Palay 1963; Kohno 1969; McNutt 1978; Bruni and Reddy 1987), it is still difficult to imagine how F-actin is organized into a ring-like structure in the central canal but an uninterrupted belt-like network in the choroid plexus.

Although the most abundant cytoskeletal component, F-actin is extraordinarily difficult to study by morphological techniques because of its small size and its sensitivity to fixation and dehydration (Small 1981; Hirokawa et al. 1982). At present, phalloidin, a mushroom-derived toxin, is widely acknowledged as a highly specific probe for F-actin because it recognizes filamentous actin but not free actin monomers (Wulf et al. 1979). Correspondingly, a few methods using this probe have been previously developed to study the ultrastructural organization of F-actin (Lachapelle and Aldrich 1988; Castellani-Ceresa et al. 1991,1992; Deerinck et al. 1994; Capani et al. 2001). Several researchers have reported the use of an FITC-anti-FITC system to detect F-actin at the EM level (Castellani-Ceresa et al. 1991,1992). This F-actin detection method was employed here, because both FITC-conjugated

phalloidin and anti-FITC antibodies are now commercially available. Moreover, FITC-labeled materials and protocols can be used for both light microscopy and EM studies (van Dam et al. 1991), thereby serving the purpose of this study.

In the present study, we used double-fluorescence labeling to further examine the localization of F-actin and the spatial relation of F-actin to the other cytoskeletal components in ependymocytes. Thereafter, we tried to convert fluorescence signals for F-actin to peroxidase/DAB reaction products by incubating the FITC-labeled sections with a biotinylated anti-FITC antibody followed by enhancement using the avidin–biotin–peroxidase complex (ABC) method. The central canal and choroid plexus were used here because they have been widely studied and well defined at the EM level.

Materials and Methods

Animals

A total of seven female adult Sprague-Dawley rats (400–450 g; CLEA Japan Ltd., Tokyo, Japan) were used in the present study. This choice was approved by the RIKEN Experimental Animal Committee. The work was performed in accordance with the Guide for the Care and Use of Laboratory Animals (National Academy Press, Washington, 1996).

Fluorescence Microscopic Studies

Three rats were perfused through the heart with 50 ml physiological saline under diethyl ether anesthesia, followed by 200–300 ml 4% paraformaldehyde in 0.1 M phosphate buffer (PB), pH 7.4. Cervical segments of spinal cord and diencephalons containing diencephalic choroid plexus were dissected out, postfixed in the same fixative for 2–6 hr at 4C, and then washed in a series of cold sucrose solutions of increasing concentration. The samples were embedded in OCT compound (Tissue-Tek; Sakura Finetek Japan Co. Ltd., Tokyo, Japan), frozen on dry ice, then cut into 40-μm-thick transverse sections using a freezing microtome (Yamato, Japan).

Immunohistochemistry was performed on free-floating sections. The cryosections were preincubated with 3% normal goat serum in 0.1 M PB containing 0.1% Triton X-100 for 30 min at room temperature and then incubated with primary antibodies overnight at 4C. A monoclonal anti–α-tubulin antibody (Clone DM1A; Sigma Chemical, St. Louis, MO) was used to examine microtubules. A monoclonal anti-vimentin antibody (Clone V9; Sigma) was used to detect vimentin intermediate filaments. A guinea pig polyclonal antibody against cytokeratins 8/18 (GP11; PROGEN Biotechnik GmbH, Heidelberg, Germany) and a monoclonal anti–pan cytokeratin mixture (of clones C-11, PCK-26, CY-90, KS-1A3, M20, and A-53-B/A2; Sigma) were used to examine cytokeratin intermediate filaments. As control, the primary antibodies were replaced with 0.1 M PB.

After several washes with 0.1 M PB, the sections were reacted with Alexa Fluor–conjugated secondary antibodies (Molecular Probes; Eugene, Oregon) and 2 μg/ml FITC-conjugated phalloidin (p5282; Sigma) in 0.1 M PB for 1 hr, and then reacted with 0.5 μg/ml 4′-6-diamidino-2-phenylindole (DAPI; Nacalai Tesque, Kyoto, Japan) in 0.1 M PB for 5 min at room temperature. The Alexa Fluor–conjugated secondary antibodies used here included Alexa 594–conjugated goat anti-guinea pig IgG antibody for guinea pig anti-cytokeratin 8/18 antibody and Alexa 594–conjugated goat anti-mouse IgG antibody for monoclonal anti–α-tubulin antibody, monoclonal anti-vimentin antibody and anti–pan cytokeratin antibody. DAPI was used here to stain the nucleus.

The sections were mounted onto glass slides with Immu-Mount (Shandon; Pittsburgh, PA), and examined with a laser scanning confocal microscope (Olympus FV1000; Olympus, Tokyo, Japan) under excitation wavelengths of 358 nm for DAPI, 488 nm for FITC, and 594 nm for Alexa 594, respectively.

EM Detection of F-actin

Four rats were fixed and dissected as described above. Cervical segments of spinal cord and diencephalons were postfixed in fresh fixative for 4–6 hr, then left in 0.1 M PB containing 5% sucrose overnight at 4C. The samples were cut into 50-μm-thick sections on a DSK microslicer (DTK-1000; Ted Pella, Dosaka EM, Kyoto, Japan).

Some sections were pretreated with 3% H_2O_2 in 0.1 M PB for 30 min before blocking to extinguish endogenous peroxidase. The blocking solution contained 0.5% bovine serum albumin (Sigma), 0.1% cold-water fish gelatin (Sigma), and 0.02% saponin (Nacalai Tesque) in 0.1 M PB (pH 7.4). Blocking for 1 hr was followed by an overnight incubation with 4 μg/ml FITC-conjugated phalloidin in 0.1 M PB rinse buffer (pH 7.4), containing 0.1% cold-water fish gelatin and 0.02% saponin, at 4C.

After thorough washes, the sections were mounted onto glass slides with a drop of 0.1 M PB, and examined at 488-nm excitation with the Olympus confocal laser microscope. Thereafter, the sections were soaked in 0.1 M PB, and removed from the glass slides. After additional washes, the sections were incubated with biotinylated mouse anti-FITC antibody (1:50, Clone FL-d6; Sigma) in 0.1 M PB rinse buffer for 2 days at 4C, and then processed with ABC for 1 hr at room temperature, according to the manufacturer's instructions (Vectastain ABC Kit; Vector Laboratories, Burlingame, CA). The sections were stained for peroxidase activity by preincubation in 0.05% DAB (Sigma) in 0.05 M Tris-HCl buffer (pH 7.2). After 30 min, the incubation medium was exchanged for fresh DAB solution containing

0.01% H_2O_2 and incubated on a shaker for an additional 15 min. The peroxidase/DAB reaction was stopped by three 10-min washes in 0.05 M Tris-HCl buffer followed by three more 10-min washes in 0.1 M PB.

The specificity of the staining for F-actin was verified by incubating sections by omitting FITC-conjugated phalloidin and by omitting the anti-FITC antibody. DAB-stained sections were photographed using a light microscope equipped with a digital camera (Eclipse; Nikon, Tokyo, Japan).

Some DAB-stained sections were fixed in 2.25% glutaraldehyde in 0.1 M PB containing 0.2% tannic acid for 1 hr, and then postfixed with 0.75% OsO_4 in 0.1 M PB (pH 6) for 1 hr at 4C. This treatment has been recommended to protect F-actin from destabilizing during osmication and dehydration (Fifková and Delay 1982; Capani et al. 2001). After a brief wash with distilled water, the DAB sections and some unstained sections were dehydrated in increasing concentrations of ethanol and embedded in Epon 812.
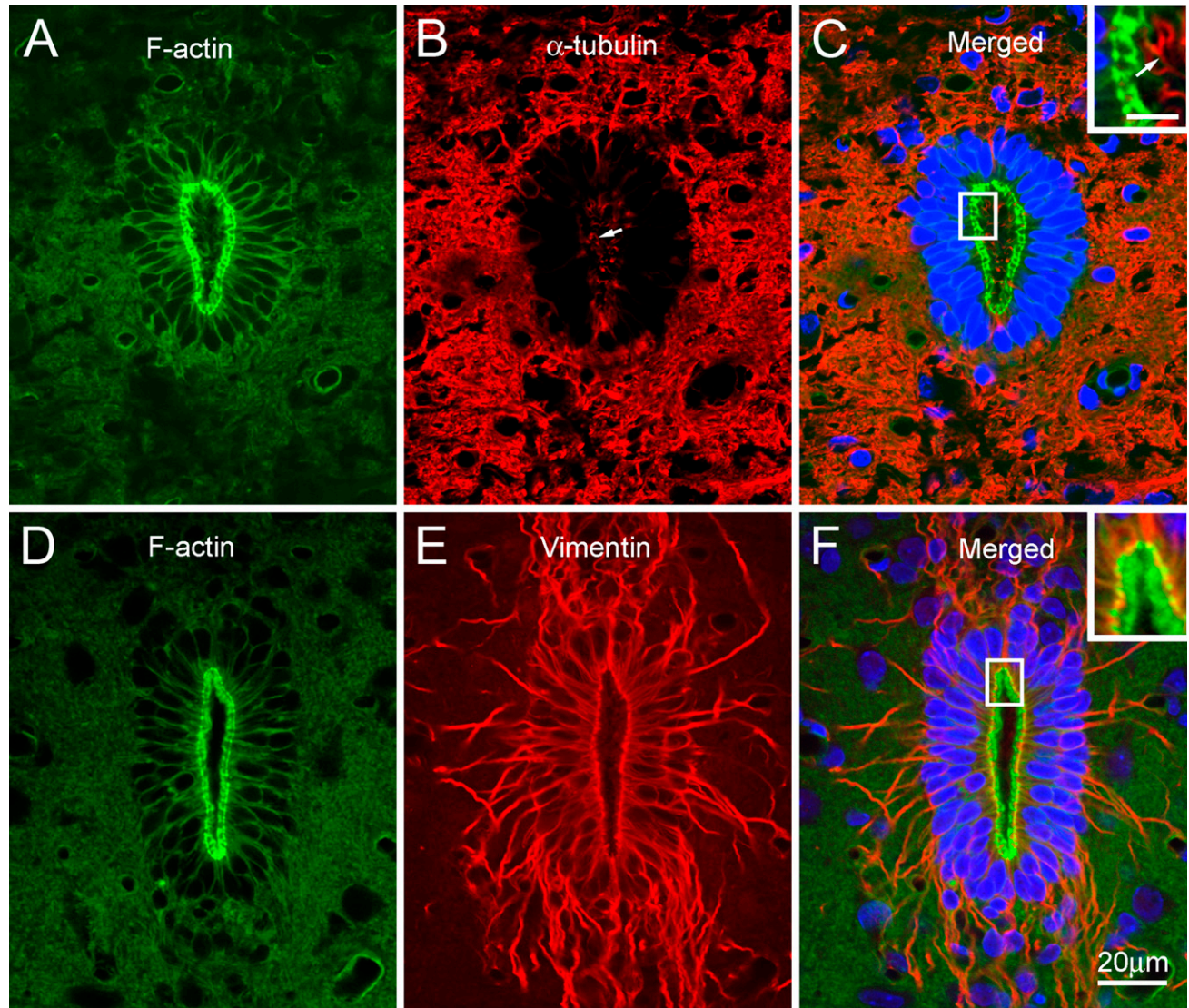
Figure 1 Fluorescence microscopic localization of F-actin, α-tubulin, and vimentin in the central canal. The ependymocytes of the central canal contain peripherally distributed F-actin (**A,D**). In the apical region, F-actin is arranged into a ring-like structure surrounding the lumen of the central canal. The lateral cell margins are also less intensely labeled. Positive signals for α-tubulin are seen predominantly in the apical region of the central canal, where they are present in the cytoplasmic protrusions of the ependymocytes (arrow in **B**). **C** is merged from **A** and **B**. No F-actin labeling is found in the α-tubulin–positive structures protruding into the lumen (arrow in **C**). Nuclei were stained blue with 4'-6-diamidino-2-phenylindole (DAPI). Vimentin-positive components are organized into a polarized network in the central canal (**E**). In the apical region, vimentin filaments run circumferentially beneath the apical F-actin network. Basally, they extend along the peripheral processes of ependymocytes into the subependymal zone with a root-like appearance. **F** is merged from **D** and **E**. The inset shows the colocalization (yellow color) of vimentin with F-actin in the outer boundary of the F-actin ring. Nuclei were stained blue with DAPI. Bar in inset = 5 μm.

Ultrathin sections ~100 nm thick were cut on an ultracut E ultramicrotome (Reichert-Jung Optische Werk AG; Wien, Austria), and collected on Formvar-coated slot grids. Ultrathin sections from the unstained samples were stained with 4% uranyl acetate and 0.3% lead citrate, and examined with a transmission electron microscope (Tecnai 12; FEI, Hillsboro, OR). The DAB-labeled samples were examined without heavy metal contrasting. EM images were recorded on Image Plates (FujiFilm; Tokyo, Japan), which were scanned with Fujifilm FDL 5000 and converted into digital images with the software program Image Gauge V4.0 (FujiFilm).

Results

Fluorescence Microscopic Studies on F-actin, Microtubules, and Intermediate Filaments in the Ependymocytes

In the central canal, the apical region of the ependymocytes was intensely stained with FITC-conjugated phalloidin (Figures 1A and 1D). In transversely cut sections, apically localized F-actin formed a ring-like structure, surrounding the lumen of the central canal. Fluorescence signals were also observed less intensely along the lateral cell margins.

α-Tubulin in the central canal was located mainly in the cytoplasmic protrusions of ependymocytes (Figure 1B). Double labeling showed that the positive structures protruding into the lumen did not contain F-actin (Figure 1C). Cytokeratins were not demonstrated immunocytochemically in the central canal with either anti-cytokeratin 8/18 or anti–pan cytokeratin antibodies (not shown). Instead, vimentin was found as the major intermediate filamentous component (Figure 1E). Apically localized vimentin filaments ran circumferentially beneath the apical F-actin network, and partially overlapped in the outer boundary of the F-actin ring (Figure 1F). From this circumferential network, vimentin filament bundles radiated into the subependymal zone and formed a root-like structure.
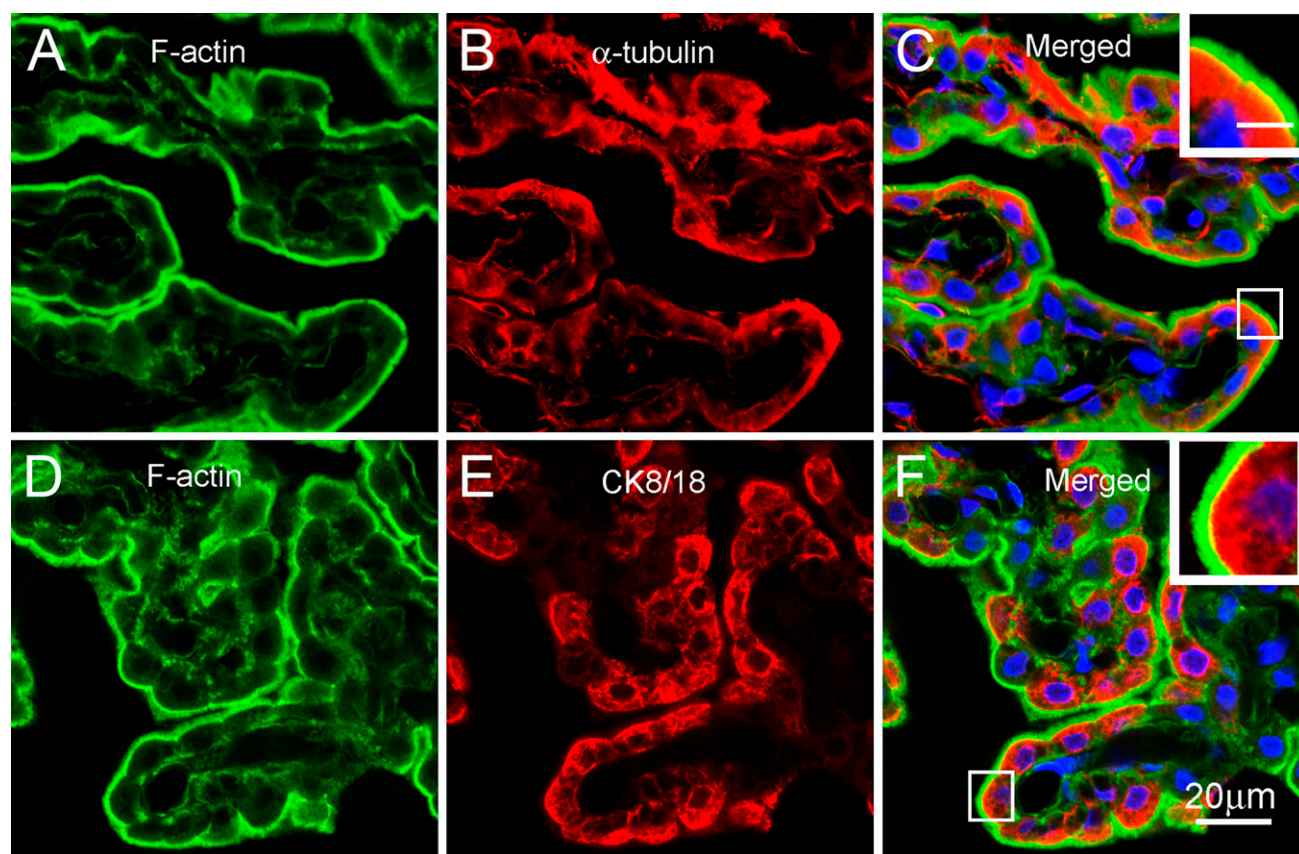

Figure 2 Fluorescence microscopic localization of F-actin, α-tubulin, and vimentin in the choroid plexus. In the choroid plexus, F-actin is localized predominantly in the apical region, appearing as a bright uninterrupted belt along the luminal surface (**A,D**). Less-intense labeling is also noted in the stroma of the choroid plexus. The perinuclear cytoplasm of ependymocytes was positive for anti–α-tubulin (**B**) and anti–cytokeratin antibody (**E**). **C** is merged from **A** and **B**, showing that almost no protrusions positive for α-tubulin are present on the luminal surface. The inset shows a partial colocalization (yellow color) of α-tubulin with F-actin in the periphery of the F-actin network. Nuclei were stained blue with DAPI. **F** is merged from **D** and **E**. The inset shows a partial colocalization (yellow color) of cytokeratin with F-actin in the periphery of the F-actin network. Nuclei were stained blue with DAPI. Bar in inset = 5 μm.

In the choroid plexus, FITC–phalloidin staining revealed a smooth and uninterrupted bright belt along the apical border (Figures 2A and 2D). The cytoplasm of the ependymocytes was rarely stained, but there were a few fluorescence signals in the stroma of the choroid plexus. The perinuclear cytoplasm of the choroidal ependymocytes was intensely labeled with anti–α-tubulin antibody (Figure 2B), but protrusions positive for α-tubulin were rarely observed on the luminal surface of the choroid plexus (Figure 2C). Cytokeratins 8/18 were found as the main intermediate filamentous component in the choroid plexus, and were localized in the perinuclear cytoplasm of the choroidal ependymocytes (Figure 2E). On the other hand, positive signals for vimentin were observed only in the stroma but not in the choroidal ependymocytes (not shown). Double labeling

showed that both α-tubulin and cytokeratins were distributed beneath the apical F-actin network, with a partial colocalization with F-actin in the periphery of the apical F-actin network (Figures 2C and 2F).

EM Localization of F-actin in the Ependymocytes

By use of a phalloidin-based FITC-anti-FITC method, fluorescence labeling of F-actin was converted to a DAB reaction product visible by light microscopy. The overall distribution of reaction products for F-actin agreed well with that obtained by FITC-conjugated phalloidin staining and confocal microscopy (Figures 3 and 4). The specificity of this conversion was further confirmed by omitting FITC-conjugated phalloidin (Figures 3A and 3E) or by omitting the anti-FITC antibody (Figures 3B and 3F) in the immunostaining procedure.
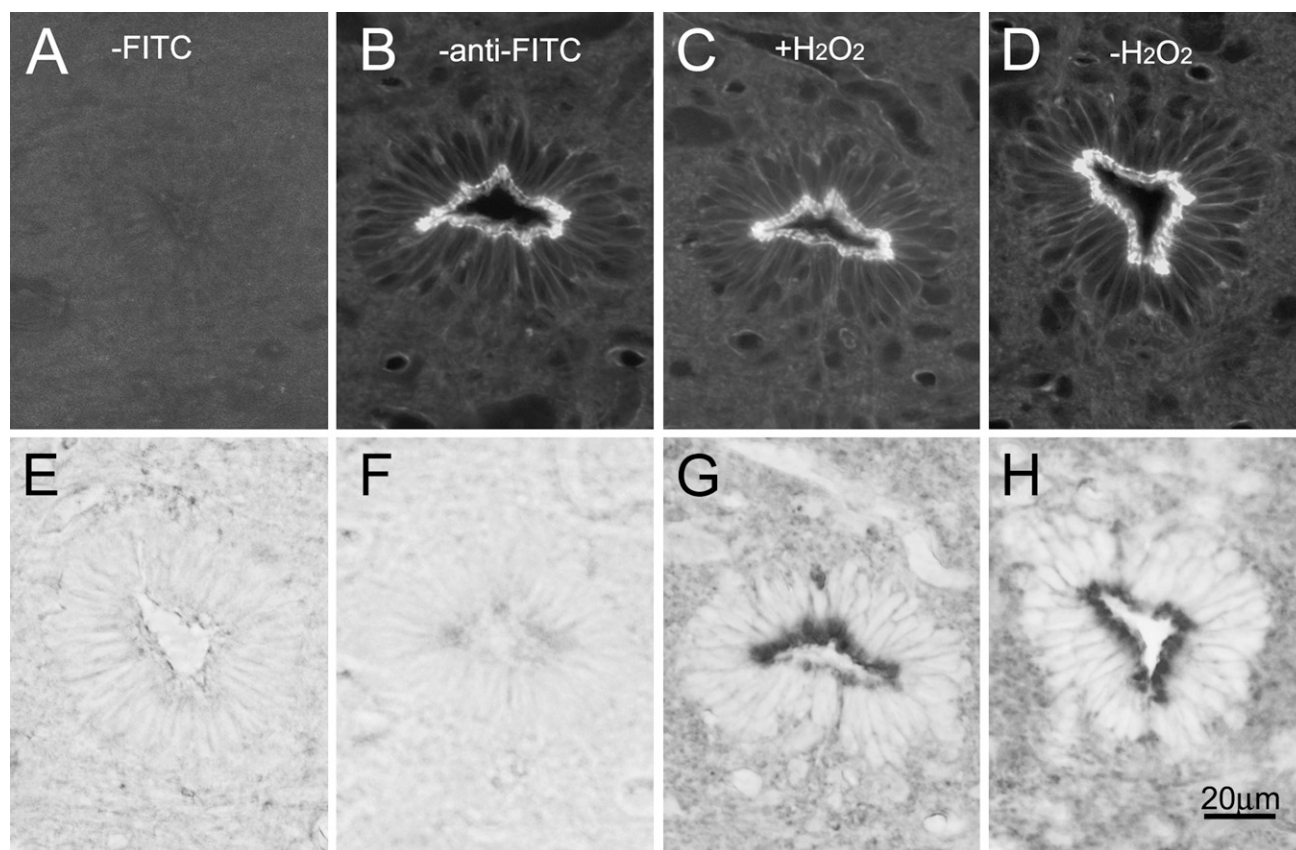

Figure 3 Comparison of F-actin staining in the central canal between fluorescence and light microscopic images. The panels in the upper and lower row show fluorescence and light microscopic images, respectively. It is worth mentioning that confocal laser scanning microscopy can visualize F-actin clearly with no interference due to out-of-focus noise. (**A,E**) No fluorescence signals are detected when FITC-conjugated phalloidin is replaced with 0.1 M phosphate buffer (PB) rinse buffer (**A**). The same section is subsequently incubated with biotinylated anti-FITC antibody, followed by detection with the avidin–biotin–peroxidase complex (ABC) method. However, this does not reveal any positive labeling in the central canal (**E**). (**B,F**) FITC-conjugated phalloidin staining reveals a ring-like network in the central canal (**B**). F-actin is directly detected in the same section using the ABC method. No peroxidase/DAB reaction products are observed in the central canal (**F**). (**C,G**) Fluorescence signals for F-actin are detectable after pretreatment with 3% H_2O_2 in 0.1 M PB (**C**). The same section is then reacted with biotinylated anti-FITC antibody, followed by detection using the ABC method. Peroxidase/DAB reaction products are found predominantly in the apical region of the central canal (**G**). (**D,H**) FITC-conjugated phalloidin staining reveals a ring-like network in the central canal in the section without pretreatment with H_2O_2 (**D**). The same section is then reacted with biotinylated anti-FITC antibody, followed by detection using the ABC method. Peroxidase/DAB reaction products are localized predominantly in the apical region of the central canal (**H**). It is noted that no discernable differences in the distribution of F-actin are found in the sections pretreated with and without H_2O_2.
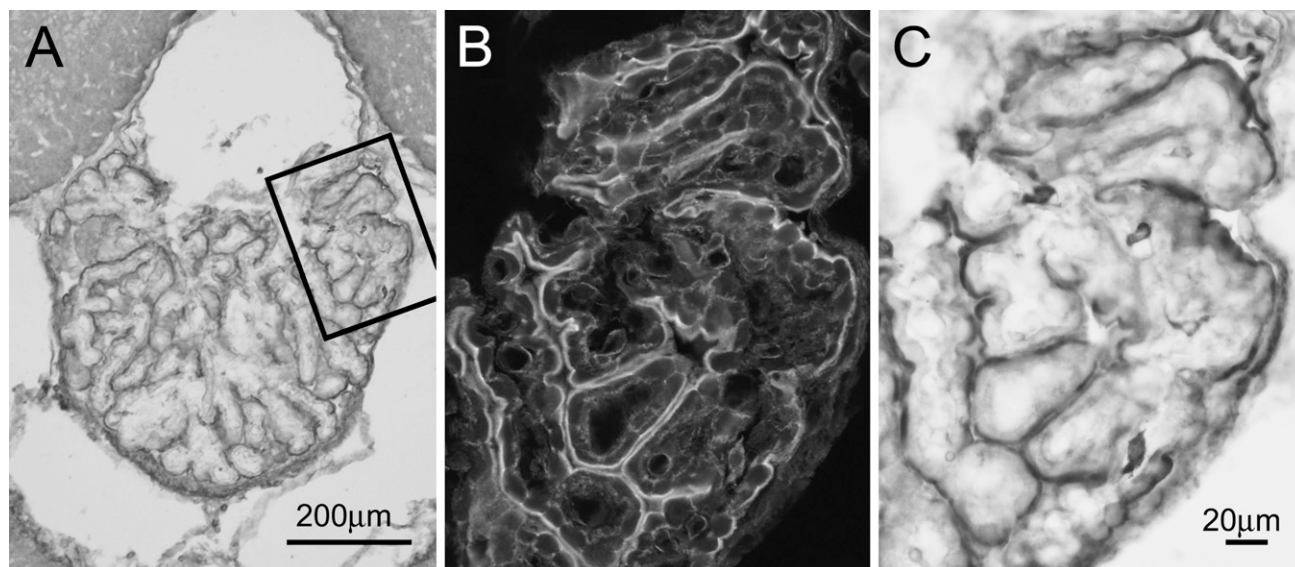
Figure 4 Comparison of F-actin staining in the choroid plexus between fluorescence and light microscopic images. **(A)** Distribution of peroxidase/DAB reaction products for F-actin in the diencephalic choroid plexus, revealed by use of the phalloidin-based FITC-anti-FITC technique. The area within the rectangle in **A** is enlarged in **B** and **C** to show fluorescence and DAB labeling, respectively. Bar in **C** applies to **B**.

The apical region of the ependymocytes was intensely labeled with peroxidase/DAB reaction products in both the central canal (Figure 3) and the choroid plexus (Figure 4). As observed by confocal microscopy, the lateral cell margins in the central canal showed less-intense staining. Almost no discernable differences in the distribution of F-actin were noted in the samples pre-treated with (Figures 3C and 3G) and without H_2O_2 (Figures 3D and 3H); however, the use of hydrogen peroxide often resulted in the folding of sections. Therefore, the results obtained from the samples without H_2O_2 treatment were presented here. Alternatively, unstained samples were used as negative control.

Under the electron microscope, the reaction products for F-actin were localized mainly in the apical aspects in the central canal (Figure 5). Microvilli were intensely labeled from the tip downward into the apical cytoplasm. Beneath the microvilli, there was an intensely labeled F-actin network running circumferentially and associated with the cytoplasmic sides of intermediate junctions (Figures 5A, 5C, and 5D). The cytoplasmic sides of intermediate junctions showed a darkened thickening (arrowhead in Figure 5D).

By comparing fluorescence and EM images, the circumferential F-actin network, the so-called terminal web, was found as the structural equivalent of the outer boundary of the F-actin fluorescence ring, whereas the width of the fluorescence ring defined at the light microscopic level was shown to be the distance between the terminal web and the tip of the microvilli (Figures 5A and 5B).

Not the whole cytoplasm between microvilli and the terminal web was completely labeled. The distal portion of cilia protruding into the lumen was rarely stained (Figure 5A), but basal bodies displayed a darkened appearance (Figure 5C). Intermediate filaments were unlabeled, but they were found to frequently loop up and connect to the circumferential F-actin bundles (Figure 5D).

On the other hand, no labeling was found in the negative control, although the terminal web was also visible in the apical region of the central canal (Figure 6). Blood vessels of various sizes present in the gray matter of the spinal cord showed complete labeling for F-actin under the confocal microscope, and were therefore used as positive control. Examination of capillaries at the ultrastructural level revealed continuous intense labeling in the luminal border of endothelial cells (Figure 7).

In the choroid plexus, microvilli were intensely labeled, whereas staining was relatively rare in the remaining cytoplasm (Figure 8A). The choroidal ependymocytes were characterized by a large number of pleomorphic microvilli that showed bulbous ends at their apexes. F-actin labeling was found along the length of the microvilli, but was often absent at the center of their bulbous ends. Cilia or junctional membrane thickenings were rarely encountered. Although there was patchy staining extending beneath the microvilli at their bases, there was no appreciable terminal web beneath the microvilli (Figures 8B and 8C). These were also confirmed in the negative control (Figure 8D).

Discussion

The cytoskeleton in living cells is composed of three separate filamentous networks: microfilaments, micro-
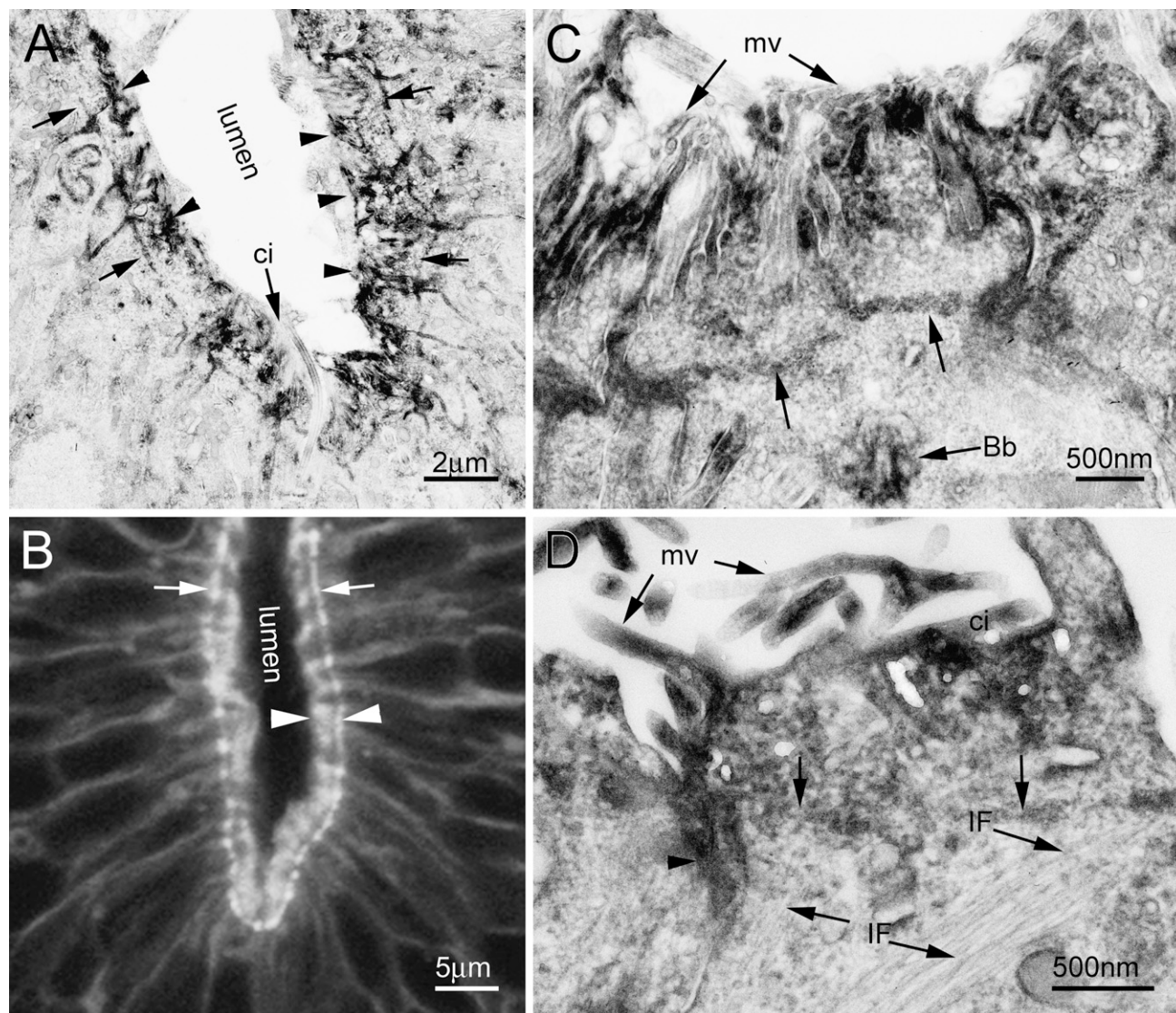
Figure 5 Ultrastructural localization of F-actin in the central canal. The electron microscopic (EM) image in **A** gives an overview of the distribution of F-actin in the central canal at low magnification. The peroxidase/DAB reaction products for F-actin are localized predominantly in the apical aspects in the central canal, with only a diffuse staining in the remaining cytoplasm. In the apical region, microvilli (arrowheads in **A**; see **C** and **D** for more detail) are found as the major component positive for F-actin. Beneath the microvilli, a circumferential F-actin network (arrows) runs parallel to the apical surface of the ependymocytes by associating with the plasmalemma thickenings between adjacent cells. Notably, the labeling for F-actin is not even in the cytoplasm between microvilli and the circumferential F-actin network. A cilium (arrow indicated by ci) is also seen protruding into the lumen of the central canal, but its shaft shows little labeling for F-actin. (**B**) Fluorescence image of F-actin in the central canal. Arrows indicate the outer boundary of the F-actin ring. The distance between the two arrowheads has previously been defined as the width of the apical F-actin network. By comparing the fluorescence and EM images, the circumferential F-actin network (i.e., the terminal web, arrows in **A**) is found as the structural equivalent to the outer boundary of the F-actin fluorescence ring (arrows in **B**), whereas the distance between the terminal web and the tip of the microvilli corresponds to the width of the fluorescence ring. (**C,D**) Apical region of ependymocytes at higher magnification. The apical surface of the ependymocytes is covered with a profusion of microvilli (arrows labeled by mv). Microvillous cores are labeled from the tip downward to the apical cytoplasm, where they are seen frequently connected to an intensely labeled circumferential F-actin network (arrows). The cytoplasmic sides of intermediate junctions show a darkened thickening (arrowhead). A basal body (Bb), which shows a darkened appearance, is seen in **C**. Intermediate filaments (arrows labeled by IF) are unlabeled, but they frequently loop up and connect to the circumferential F-actin bundles (**D**).

tubules, and intermediate filaments (Bray and White 1988; Hollenbeck et al. 1989). Fluorescence microscopic studies showed that F-actin shares a similar localization and arrangement in the central canal and choroid plexus in the rat. In both types of ependymocytes, the apical F-actin network is further associated with the underlying intermediate filaments. A similar phenomenon has already been noted in intestinal epithelial cells (Hirokawa et al. 1982). Because the F-actin–rich cortex is able to exert a pull on all components associated with
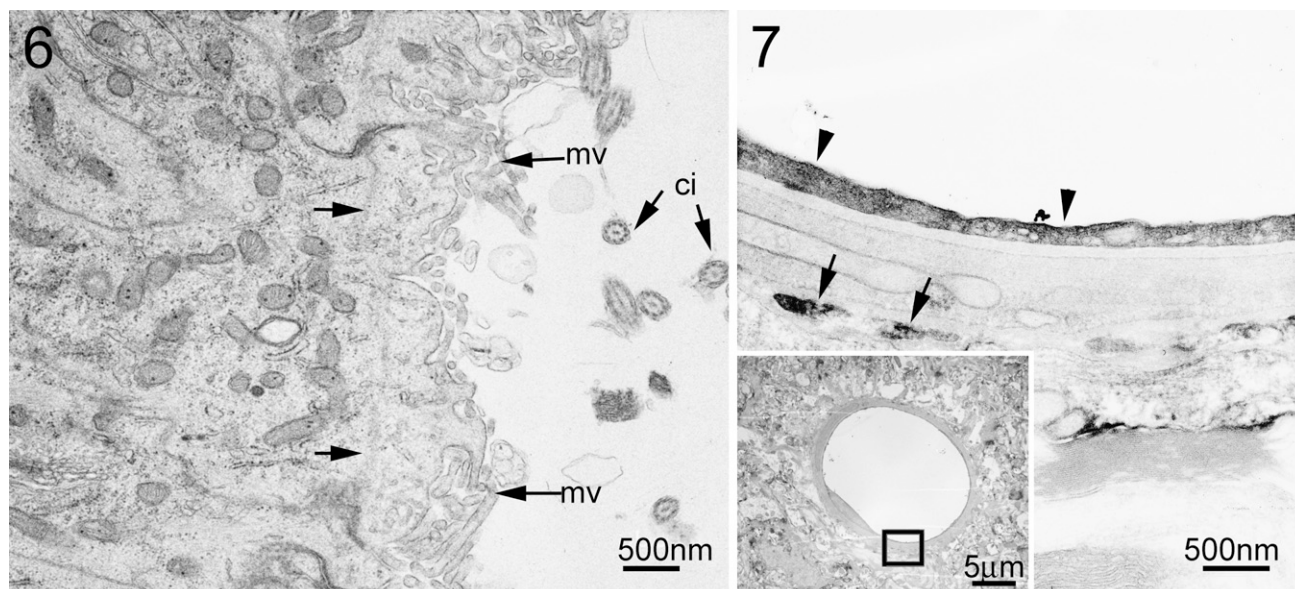
Figures 6 and 7

Figure 6 EM image from negative control. No labeling is found in the apical region of the central canal of the negative control. The apical surface of the ependymocytes is characterized by a profusion of microvilli (mv) and a varying number of cilia (ci, transverse-cut in this section). Terminal web (arrows) is discernable spanning between the neighboring junctions.

Figure 7 EM image showing a portion of a capillary (inset). Intense labeling for F-actin is seen continuously in the luminal border of the endothelial cell (arrowheads). Sporadic labeling is also observed in the perivascular glial endfeet (arrows).

it, the association between F-actin and intermediate filaments in the apical cytoplasm is suggested to play an important role in maintaining the integrity of epithelial cells (Bray and White 1988; Hollenbeck et al. 1989).

On the other hand, there are several differences in the cytoskeletal composition and organization in the two types of cells. First and most important, the ependymocytes in the central canal contain only vimentin but not cytokeratin, unlike the choroidal ependymocytes, although both cytokeratins 8/18 and vimentin have been reported in the walls of the rat cerebral ventricles (Miettinen et al. 1986; Kasper 1992). Vimentin filaments are arranged into a polarized network in the central canal, whereas cytokeratins are more evenly distributed in the perinuclear cytoplasm in the choroidal ependymocytes. Second, microtubule-containing protrusions are much more abundant in the central canal, but rarely observed in the choroid plexus. This is consistent with the fact that choroidal ependymocytes are covered with sparse cilia (Del Bigio 1995). Moreover, although F-actin is localized predominantly in the apical cytoplasm of ependymocytes, the apical F-actin in the central canal has a ring-like appearance, apparently different from the smooth and uninterrupted organization of that in the choroid plexus.

To define more precisely the localization of F-actin, fluorescence labeling of F-actin was converted to peroxidase/DAB products by using the phalloidin-based FITC-anti-FITC technique. Subsequent examination of the DAB-stained sections by EM revealed that the distribution of reaction products displays the same pattern as the fluorescence signals for F-actin.

Consistent with the light microscopic observations, F-actin is localized predominantly on the luminal surface of both types of ependymocytes. In the central canal, microvilli and terminal web were found as the main components of the positive structures. F-actin bundles extend from the tip of microvilli downward into the apical cytoplasm, and are anchored to a circumferentially running F-actin network in the terminal web. It is such organization that gives rise to a ring-like appearance in the central canal. In the choroid plexus, however, no apparent terminal web is observed beneath microvilli, whereas intensely labeled microvilli are more densely arranged on the apical surface. Comparison of fluorescence and EM images suggested that the width of the apical F-actin network reported previously can be accounted for largely by the height of the microvilli.

Microvilli and terminal web are known as F-actin-rich structures in ciliated epithelial cells (Hirokawa et al. 1982; Hagen and Trier 1988). Although the presence of microfilaments has already been ultrastructurally demonstrated in the apical cytoplasm of ependymocytes (Brightman and Palay 1963; Kohno 1969; McNutt 1978; Bruni and Reddy 1987), the ultrastructural findings presented here have been successfully correlated to
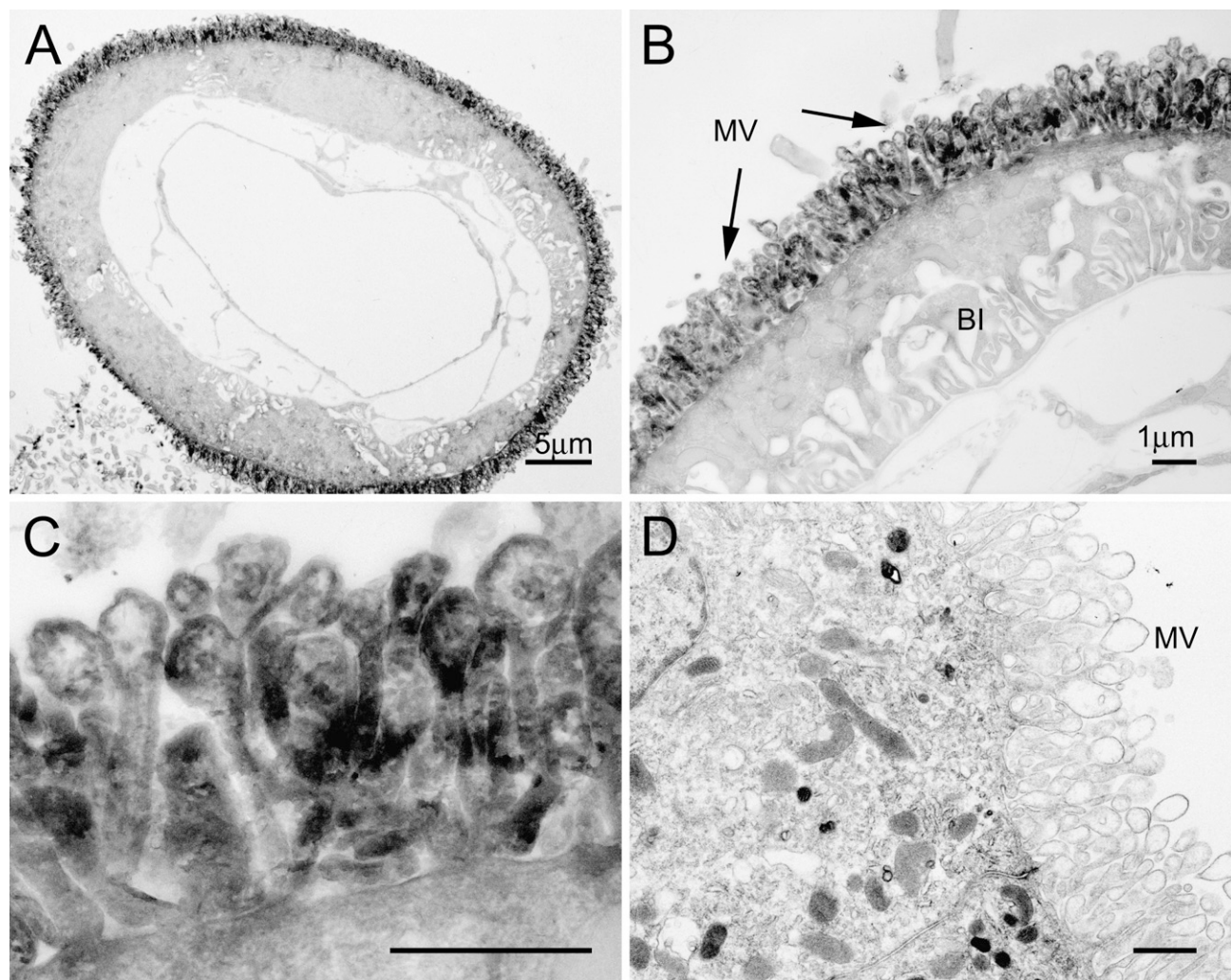
Figure 8 EM images showing the localization of F-actin in the choroid plexus. The apical regions of the choroid ependymocytes are intensely stained with the peroxidase/DAB reaction products, whereas the staining is relatively rare in the remaining cytoplasm (**A,B**). BI, basal infoldings. Labeling is observed along the whole length of the microvilli, but is often absent in the center of their bulbous ends (**B,C**). Cilia or junctional membrane thickenings are not observed. Although there is patchy staining beneath the microvilli at their base, no apparent terminal web is seen beneath the microvilli (**C**). (**D**) Apical region of a choroidal ependymocyte from negative control. The luminal border of the ependymocyte is covered with numerous pleomorphic microvilli, most of which have an electron-lucent center in their bulbous ends. No apparent circumferentially running F-actin bundles are seen beneath the microvilli. Bars: **B–D** = 1 μm.

the light microscopic results, therefore making it possible to infer the functional meaning of the apical F-actin network reported in the ventricular system.

In adult rats, we previously described a regionally varying F-actin network along the apical surface in the ventricular system using FITC–phalloidin staining and confocal laser scanning microscopy (Li et al. 2007). By comparing the width of the apical F-actin network, we found that F-actin was most prominent in the lower cervical canal and significantly differed between the ventral and dorsal aspects above the medullary canal. Recently, we further examined the postnatal development of F-actin in the central canal, and found that the apical F-actin network increased in

width after birth, and peaked in the third postnatal week (Li et al. 2008). No regional differentiation of F-actin was observed if the intervertebral spine movements of weanling rats were continuously restrained, suggesting that the organization of F-actin in the central canal is related to the postnatal development of vertebral motions.

According to the EM data available, microvilli do display regional differences along the ventricular system with respect to height as well as shape and density (Fleischhaller 1972; Ferraz de Carvalho and Costacurta 1976; Walsh et al. 1978; Yoshioka et al. 1985). For example, the dorsal wall of the cerebral ventricles above the medullary canal is often covered with scanty and

short microvilli (Walsh et al. 1978; Yoshioka et al. 1985), whereas the luminal surface of the central canal and choroid plexus is generally characterized by a profusion of stout microvilli (Bruni and Reddy 1987; Del Bigio 1995). Although postnatal development of microvilli has not been reported in the central canal, a similar postnatal increase in height and number of microvilli has already been noted in the choroid plexus in the rat fourth ventricles (Keep et al. 1986). Because choroid ependymocytes are specialized for secretion of cerebrospinal fluid, the increase in the number and height of microvilli has been thought to be an instrumental adaptation (Keep et al. 1986; Gabrion et al. 1996; Mani-Ponset et al. 1997; Davet et al. 1998).

A variety of evidence, obtained mainly by studying other ciliated epithelium systems, has shown that microvilli can adapt to altered gravity, hydrostatic pressure, or flow rate by changing their shape, size, and number (Tilney and Cardell 1970; Maunsbach et al. 1987; Gabrion et al. 1996; Mani-Ponset et al. 1997; Davet et al. 1998; Doughty 1998). Therefore, it is possible that the microvilli of the ependymocytes may have a similar capability and are therefore able to organize themselves according to the differing demands of differently positional cells against external forces.

Unlike their counterparts in the central canal, the microvilli in the choroidal plexus contain a loose F-actin network that does not form a well-developed terminal web beneath the microvilli (McNutt 1978). Previously, Kohno (1969) has noted the presence of pronounced cross-striated microfilaments in the apical aspects of the central canal, which are now known as the so-called terminal web. Because similar structures are lacking or are less well developed in the cerebral ventricles, several authors have suggested that such structures act as a support that protects the lumen of the canal from collapsing during compression generated by movements of the spine (Brightman and Palay 1963; Kohno 1969; Bruni and Reddy 1987; Li et al. 2007,2008). These studies provided ultrastructural evidence showing that the F-actin bundles in the terminal web span the entire circumference of the central canal by associating with the intermediate junctions between adjacent cells. This circumferential F-actin network is further enforced by the underlying vimentin intermediate filaments. Our observations suggest that the apical F-actin, together with the intermediate filaments, is capable of transmitting tension from one cell to another, therefore playing a role in maintaining the structural integrity of the central canal.

Acknowledgments

Literature Cited

Bray D, White JG (1988) Cortical flow in animal cells. Science 239:883–888

Brightman MW, Palay SL (1963) The fine structure of ependyma in the brain of the rat. J Cell Biol 19:415–439

Bruni JE, Reddy K (1987) Ependyma of the central canal of the rat spinal cord: a light and transmission electron microscopic study. J Anat 152:55–70

Capani F, Deerinck TJ, Ellisman MH, Bushong E, Bobik M, Martone ME (2001) Phalloidin-eosin followed by photo-oxidation: a novel method for localizing F-actin at the light and electron microscopic levels. J Histochem Cytochem 49:1351–1361

Castellani-Ceresa L, Brivio MF, Radaelli G (1991) Electron microscopic localization of F-actin in acrosome reacted boar spermatozoa by means of a phalloidin-FITC complex. J Submicrosc Cytol Pathol 23:347–349

Castellani-Ceresa L, Brivio MF, Radaelli G (1992) F-actin in acrosome-reacted boar spermatozoa. Mol Reprod Dev 33:99–107

Davet J, Clavel B, Datas L, Mani-Ponset L, Maurel D, Herbuté S, Viso M, et al. (1998) Choroidal readaptation to gravity in rats after spaceflight and head-down tilt. J Appl Physiol 84:19–29

Deerinck TJ, Martone ME, Lev-Ram V, Green DP, Tsien RY, Spector DL, Huang S, et al. (1994) Fluorescence photooxidation with eosin: a method for high resolution immunolocalization and in situ hybridization detection for light and electron microscopy. J Cell Biol 126:901–910

Del Bigio MR (1995) The ependyma: a protective barrier between brain and cerebrospinal fluid. Glia 14:1–13

Doughty MJ (1998) Changes in cell surface primary cilia and microvilli concurrent with measurements of fluid flow across the rabbit corneal endothelium ex vivo. Tissue Cell 30:634–643

Ferraz de Carvalho CA, Costacurta L (1976) Ultrastructural study on topographical variations of the ependyma in Bradypus tridactylus. Acta Anat (Basel) 94:369–385

Fifková E, Delay RJ (1982) Cytoplasmic actin in neuronal processes as a possible mediator of synaptic plasticity. J Cell Biol 95:345–350

Fleischhaller K (1972) Ependyma and subependymal layer. In Bourne GH, ed. The Structure and Function of Nervous Tissue, vol. 6. New York, Academic Press, 1–46

Gabrion J, Maurel D, Clavel B, Davet J, Fareh J, Herbuté S, O'Mara K, et al. (1996) Changes in apical organization of choroidal cells in rats adapted to spaceflight or head-down tilt. Brain Res 734:301–315

Gröschel-Stewart U, Unsicker K, Leonhardt H (1977) Immunohistochemical demonstration of contractile proteins in astrocytes, marginal glial and ependymal cells in rat diencephalon. Cell Tissue Res 180:133–137

Hagen SJ, Trier JS (1988) Immunocytochemical localization of actin in epithelial cells of rat small intestine by light and electron microscopy. J Histochem Cytochem 36:717–727

Hirokawa N, Tilney LG, Fujiwara K, Heuser JE (1982) Organization of actin, myosin, and intermediate filaments in the brush border of intestinal epithelial cells. J Cell Biol 94:425–443

Hollenbeck PJ, Bershadsky AD, Pletjushkina OY, Tint IS, Vasiliev JM (1989) Intermediate filament collapse is an ATP-dependent and actin-dependent process. J Cell Sci 92:621–631

Ishii T, Haga S, Tokutake S (1978) Immunofluorescence studies on localization of actin-like protein in the mouse brain. Acta Neuropathol 42:99–103

Kasper M (1992) Cytokeratins in intracranial and intraspinal tissues. Adv Anat Embryol Cell Biol 126:1–82

Keep RF, Jones HC, Cawkwell RD (1986) A morphometric analysis of the development of the fourth ventricle choroid plexus in the rat. Brain Res 392:77–85

Kohno K (1969) Electron microscopic studies on Reissner's fiber and the ependymal cells in the spinal cord of the rat. Z Zellforsch Mikrosk Anat 94:565–573

Koshiba K (1987) Ultrastructure of the choroid plexus epithelium of pigeons treated with drugs: II. Effect of cytochalasin D and colchicine. Am J Anat 178:133–143

Lachapelle M, Aldrich HC (1988) Phalloidin-gold complexes: a new tool for ultrastructural localization of F-actin. J Histochem Cytochem 36:1197–1202

Li YC, Bai WZ, Hashikawa T (2007) Regionally varying F-actin network in the apical cytoplasm of ependymocytes. Neurosci Res 57:522–530

Li YC, Bai WZ, Hashikawa T (2008) Postnatal reorganization of F-actin in the central canal of the spinal cord in the rat. Brain Res 1239:100–106

Mani-Ponset L, Masseguin C, Davet J, Herbuté S, Maurel D, Ghandour MS, Reiss-Bubenheim D, et al. (1997) Effects of an 11-day spaceflight on the choroid plexus of developing rats. Brain Res Dev Brain Res 99:187–200

Maunsbach AB, Giebisch GH, Stanton BA (1987) Effects of flow rate on proximal tubule ultrastructure. Am J Physiol 253: F582–587

McNutt NS (1978) A thin-section and freeze-fracture study of microfilament-membrane attachments in choroid plexus and intestinal microvilli. J Cell Biol 79:774–787

Mestres P, Garfia A (1980) Effects of cytochalasin B on the ependyma. Scan Electron Microsc 3:465–474

Miettinen M, Clark R, Virtanen I (1986) Intermediate filament proteins in choroid plexus and ependyma and their tumors. Am J Pathol 123:231–240

Peters A, Palay SL, Barster H (1991) The Fine Structure of the Nervous System: Neurons and their Supporting Cells. 3rd ed. Oxford, Oxford University Press, 312–327

Small JV (1981) Organization of actin in the leading edge of cultured cells: influence of osmium tetroxide and dehydration on the ultrastructure of actin meshworks. J Cell Biol 91:695–705

Tilney LG, Cardell RR Jr (1970) Factors controlling the reassembly of the microvillus border of the small intestine of the salamander. J Cell Biol 47:408–422

van Dam GJ, Bogitsh BJ, Fransen JA, Kornelis D, van Zeyl RJ, Deelder AM (1991) Application of the FITC-anti-FITC-gold system to ultrastructural localization of antigens. J Histochem Cytochem 39:1725–1728

Walsh RJ, Brawer JR, Lin PL (1978) Early postnatal development of ependyma in the third ventricle of male and female rats. Am J Anat 151:377–407

Wulf E, Deboben A, Bautz FA, Faulstich H, Wieland T (1979) Fluorescent phallotoxin, a tool for the visualization of cellular actin. Proc Natl Acad Sci USA 76:4498–4502

Yoshioka T, Inomata K, Tanaka O (1985) Cytochemical localization of alkaline phosphatase in the ependyma of the rat medulla oblongata. Cell Tissue Res 241:415–420